Interdisciplinary Research in Medical Sciences Specialty
ISSN: 3062-4401
2025, Volume 5, Issue 2, Page No: 113-130

Available online at: www.galaxypub.co/page/journals

Galaxy Publication

A Quantifiable CD13/CD29/CD90 Marker Panel Defines Human Mesenchymal Stem Cell–Derived Small Extracellular Vesicles

João Silva[1]*, Pedro Costa[1], Ana Beatriz[2]

[1]Department of Stem Cell Biology and Extracellular Vesicles, Faculty of Medicine, Federal University of Rio de Janeiro, Rio de Janeiro, Brazil.
[2]Department of Mesenchymal Stem Cell Research, Faculty of Pharmaceutical Sciences, University of Campinas, Campinas, Brazil.

***E-mail** ✉ joao.silva@ufrj.br

Received: 15 May 2025; **Revised:** 12 July 2025; **Accepted:** 18 July 2025

ABSTRACT

Small extracellular vesicles originating from human mesenchymal stem cells (MSC-sEVs) exhibit notable immunomodulatory and tissue-regenerative properties. Nonetheless, the absence of well-defined specific markers for these vesicles remains a critical barrier to their effective clinical deployment. In the present work, proteomic profiles of MSC-sEVs generated from three different cellular origins were examined in parallel. Candidate surface antigens commonly expressed by MSCs were identified based on their prominent representation within the MSC-sEV proteome. MSC-sEVs isolated from adipose tissue, umbilical cord, and induced pluripotent stem cells were subsequently labeled using fluorescein-conjugated antibodies and subjected to high-resolution analysis by NanoFCM at the individual vesicle level. The surface markers CD13, CD29, and CD90 displayed positive detection rates exceeding 60% across sEVs from all three MSC sources, in contrast to the generally lower rates observed for other tested candidates. These strong expression levels were further corroborated in MSC-sEVs obtained through alternative isolation procedures. Complementary validation by high-resolution microscopy confirmed the substantial presence of these markers on MSC-sEVs. Importantly, non-MSC-derived sEVs failed to show concurrent positivity for CD13, CD29, and CD90 above 40%, supporting the utility of this three-marker panel—applied with a minimum 50% positivity threshold for each marker—as a selective discriminator between MSC-sEVs and vesicles from other sources. In addition, the performance of this marker combination was monitored in sEVs released by MSCs over increasing culture passages. A progressive reduction in CD29 and CD90 positivity was observed with higher passage numbers, coinciding with diminished proliferative activity of the corresponding sEVs. Overall, this study establishes a reliable, quantifiable marker panel suitable for standardized characterization of MSC-sEVs, thereby aiding the development of robust quality control assays and supporting accelerated clinical advancement of MSC-sEV-based therapies.

Keywords: Marker identification, Mesenchymal stem cells, Proteomics, Small extracellular vesicles

How to Cite This Article: Silva J, Costa P, Beatriz A. A Quantifiable CD13/CD29/CD90 Marker Panel Defines Human Mesenchymal Stem Cell–Derived Small Extracellular Vesicles. Interdiscip Res Med Sci Spec. 2025;5(2):113-30. https://doi.org/10.51847/a9OoezqYfi

Introduction

Small extracellular vesicles (sEVs) constitute a class of cell-secreted nanoparticles measuring less than 200 nm in diameter and surrounded by a phospholipid bilayer [1, 2]. These vesicles mediate intercellular signaling by transporting a variety of bioactive molecules—such as proteins, lipids, and nucleic acids—to both nearby and remote target cells, thereby influencing recipient cell behavior and physiological processes [3-6]. In recent years, sEVs derived from human mesenchymal stem cells (MSC-sEVs) have demonstrated encouraging therapeutic benefits in preclinical models of disorders affecting multiple physiological systems, including dermal [7], musculoskeletal [8, 9], urinary [10, 11], cardiovascular [12, 13], neurological [14, 15], and immune-related conditions [16, 17]. Their beneficial actions encompass stimulation of cell proliferation and migration, prevention of programmed cell death, control of inflammation, and induction of new blood vessel formation [18, 19]. A key

advantage of MSC-sEVs over whole-cell therapies lies in their ability to bypass risks such as tumor development and embolic complications associated with stem cell transplantation [18, 20, 21]. Additional favorable attributes include limited immunogenicity, effective transit across biological barriers, and practical advantages in manufacturing and distribution [21]. These features have positioned MSC-sEVs as promising therapeutic candidates currently being evaluated in multiple clinical trials [21, 22].

For instance, Li *et al*. investigated the administration of nebulized human umbilical cord MSC-sEVs in patients suffering from pulmonary fibrosis [23]. Treatment over seven days resulted in meaningful gains in respiratory symptoms and objective lung function measures. In a separate phase I/II study, Xie *et al*. evaluated intranasal delivery of allogeneic human adipose-derived MSC-sEVs for Alzheimer's disease and reported improvements in cognitive performance after twelve weeks [15]. Registry data from ClinicalTrials.gov indicate that at least 67 trials exploring stem cell-derived sEV therapies have been initiated worldwide, many of which have reached completion or remain active. To support safe and effective clinical translation of MSC-sEVs, it is essential to define standardized parameters for their identification and quality assessment [21, 24].

The MISEV2023 guidelines outline essential steps for EV characterization, including confirmation of EV-associated markers, exclusion of non-EV contaminants, evaluation of size distribution, quantitative analysis, and morphological assessment [1]. While these parameters adequately address purity and quantity, they do not reliably establish the cellular source of the vesicles. Evidence indicates that sEVs produced by different cell types or by the same cells under varying conditions can differ substantially in molecular cargo and functional outcomes [24]. Optimal characterization of MSC-sEVs should therefore combine conventional EV analyses with the application of origin-specific markers that uniquely identify MSC-derived vesicles and distinguish them from those of non-MSC origin. Such markers would not only authenticate the source of MSC-sEV preparations but also enable precise single-vesicle quantification, laying the foundation for improved quality assurance frameworks in MSC-sEV manufacturing.

The biogenesis and secretion pathways of small extracellular vesicles (sEVs) suggest that antigens specific to their cells of origin can be transferred into the vesicles, positioning these molecules as potential identifiers for sEVs [2, 5]. Our previous studies, for instance, established that certain pluripotency-associated proteins (PODXL, OCT4, Dnmt3a, LIN28A, and SSEA4) serve as distinctive signatures for sEVs released by pluripotent stem cells [25]. Building on this concept, surface antigens characteristic of mesenchymal stem cells (MSCs) are likely to offer detectable signatures for MSC-derived sEVs. The International Society for Cellular Therapy has defined minimal criteria for multipotent mesenchymal stromal cells, requiring positive expression of CD73, CD90, and CD105, along with the absence of CD45, CD34, CD14/CD11b, CD79a/CD19, and HLA class II [26]. Additional investigations have documented further MSC surface molecules, such as CD10, CD13, CD29, CD44, CD49a, CD106, CD146, and CD166 [27-30].

Analysis of published proteomic datasets by Van Balkom *et al*. revealed frequent detection of CD73, CD90, and CD105 in MSC-sEVs, while MSC-negative markers (CD14, CD34, and CD11b) were consistently absent [31]. Ramos *et al*. reevaluated conventional flow cytometry approaches for phenotyping small EVs (<900 nm) from human bone marrow-derived MSCs (B-MSCs) and confirmed the presence of CD44, CD73, and CD90 together with the lack of CD34 and CD45 [32]. Munshi *et al*. employed bead-based flow cytometry to screen 37 known EV surface markers and MSC-related membrane proteins on B-MSC sEVs, identifying prominent expression of CD63, CD81, CD29, CD44, CD105, CD146, and MCSP [33]. Similar patterns, with the notable exception of CD146, were observed by Wiklander *et al*. in sEVs from human Tert+ immortalized B-MSCs [34].

Although these reports substantiate the incorporation of various MSC surface antigens into MSC-sEVs, several critical gaps persist. Given the wide range of MSC origins—including bone marrow, adipose tissue, umbilical cord, and additional sources [29, 35, 36]—consistency of marker expression across sEVs from different MSC types remains undetermined. Moreover, quantitative evaluations of these markers are largely absent. It is also unclear which markers can serve as dependable discriminators between MSC-sEVs and vesicles from non-MSC cells. Identifying such quantifiable and selective markers is therefore a key priority.

This study applied quantitative proteomic profiling to sEVs isolated from MSCs of adipose tissue, umbilical cord, and induced pluripotent stem cell (iPSC) origins. MSC-related surface antigens were ranked according to their relative abundance in these preparations, allowing selection of highly enriched candidates. Positive rates for each candidate were measured at the single-vesicle level across the three MSC-sEV populations. Markers achieving positive rates above 60% (CD13, CD29, and CD90) were advanced as candidate identifiers. High-resolution microscopy subsequently confirmed the localization of these candidates on MSC-sEVs. Their presence was then

evaluated on sEVs derived from six non-MSC cell types, establishing that MSC-sEVs can be clearly distinguished from non-MSC counterparts through assessment of positive rates for the selected markers. This approach led to the definition of a targeted marker panel specific to MSC-sEVs. Additionally, positive rates of CD29 and CD90 were found to decrease with advancing MSC passage numbers, paralleling a significant reduction in functional potency. These results lay the foundation for developing standardized, measurable, and reproducible methods to characterize MSC-sEV preparations, supporting their broader clinical implementation.

Materials and Methods

Cell culture and conditioned medium collection

Human adipose-derived mesenchymal stem cells from three donors (A-MSC-1, A-MSC-2, A-MSC-3) were acquired from ThermoFisher Scientific Inc. (StemPro™ Human Adipose-Derived Stem Cells, R7788115). Human umbilical cord-derived mesenchymal stem cells from three donors (U-MSC-1, U-MSC-2, U-MSC-3) were obtained from Shownin Biotechnologies Co., Ltd. (Primary hMSC, RC02003). Both A-MSCs and U-MSCs were propagated in serum-free ncMission hMSC Medium (RP02010, Shownin Biotechnologies Co., Ltd.), with conditioned medium (CM) collected at passages 3, 5, 7, 10, and 12. Three iPSC-derived MSC lines (i-MSC-1, i-MSC-2, i-MSC-3) were differentiated from human iPSC lines (nciPS01, nciPS02, and nciPS03, Shownin Biotechnologies Co., Ltd.) using an established differentiation protocol (provided in Supporting Information S1) [7-9]. These i-MSCs were maintained in the same serum-free ncMission hMSC Medium for CM harvesting. Human foreskin fibroblasts (HFF1), 293T embryonic kidney cells, lung carcinoma lines (A549, H460), and breast carcinoma lines (MCF7, MDA-MB-231) were sourced from the Stem Cell Bank of the Chinese Academy of Sciences. Non-MSC lines were cultured in Dulbecco's Modified Eagle's Medium (DMEM) supplemented with 4.5 g/L glucose (Corning) and 10% (v/v) fetal bovine serum (FBS, Gibco).

Conditioned medium was prepared by culturing cells in 75-cm² flasks with complete growth medium until ~80% confluence was reached. After removing the growth medium and performing two washes with sterile phosphate-buffered saline (PBS, Corning), cells were incubated in basal medium (ncMission basal medium for MSCs or glucose-containing DMEM for other lines). Following 48 hours, the supernatants were collected as CM for subsequent use.

Isolation of small extracellular vesicles (sEVs)

Differential ultracentrifugation

Small extracellular vesicles were isolated by differential ultracentrifugation (dUC) according to previously reported approaches [1, 37]. All spins were carried out at 4°C. The process began by distributing 150 mL of conditioned medium into 50-mL tubes, followed by centrifugation at 300 × g for 10 min to sediment dead cells. The collected supernatant was spun at 2000 × g for 20 min to remove cell debris and then at 10,000 × g for 30 min to eliminate larger vesicles. After these steps, the supernatant was passed through a 0.22-μm PES filter (Millipore, Cat# SCGPU05RE) for additional clearance of large particles. Ultracentrifugation of the filtered material was performed at 100,000 × g for 90 min with a SW 32 Ti Rotor (Beckman Coulter). The pellet obtained was resuspended in sterile PBS and subjected to a second identical ultracentrifugation run. Ultimately, the purified sEVs were resuspended in 1 mL of sterile PBS for immediate use or kept at −80°C for no longer than one month.

Sucrose density gradient centrifugation

For density gradient ultracentrifugation (DGUC), the early stages replicated the dUC workflow up to the initial ultracentrifugation of the supernatant at 100,000 × g for 90 min in a SW 32 Ti Rotor. The pellet was then redispersed in 2 mL of sterile PBS. Sucrose solutions at 60%, 50%, 40%, 30%, and 20% (w/v) were separately prepared in PBS using sucrose reagent (10021418, Sinopharm Chemical Reagent Co., Ltd.). These solutions were layered (2 mL each) in ascending order of density into Beckman Coulter tubes to create a discontinuous gradient, onto which the 2-mL sEVs suspension was gently placed [25, 38]. The assembled gradients were centrifuged at 150,000 × g for 10 h in a SW41 Ti Rotor (Beckman Coulter). Twelve fractions were gathered one by one from the top. Each fraction was brought to a volume of 12 mL with sterile PBS and underwent a second centrifugation at 150,000 × g for 2 h using the same rotor. Pellets recovered from the fractions were each resuspended in 500 μL sterile PBS ahead of further evaluation.

Size exclusion chromatography

Size exclusion chromatography (SEC) for sEVs isolation started identically to dUC until the first ultracentrifugation step at 100,000 × g for 90 min in a SW 32 Ti Rotor. The pellet was resuspended in 1 mL sterile PBS and loaded onto an Exosupur® purification column (ES914, Echo Biotech) per the manufacturer's directions. Columns were first equilibrated at room temperature for 30 min and rinsed with 20 mL sterile PBS. After sample application, elution with sterile PBS produced 20 fractions of 0.5 mL each [39]. Particle counts and protein amounts were measured across the collected fractions.

Characterization of sEVs

Morphology

Morphological examination of sEVs was conducted via transmission electron microscopy (TEM). A 10 µL volume of sEVs suspension (roughly 1×10^{10} particles/mL) was applied to a formvar-carbon coated 230-mesh copper grid (BZ110223b, Beijing Zhongjingkeyi Technology Co., Ltd.) for 5 min before excess liquid was absorbed with filter paper. The vesicles were fixed on the grid with 1% glutaraldehyde for 1 min, rinsed with deionized water, and negatively stained using 5 µL of 2% phosphotungstic acid for 1 min. Once dried, the samples were imaged on a Talos L120C G2 120 kV transmission electron microscope (ThermoFisher).

Particle concentration and size distribution

A NanoFCM system (U30, NanoFCM Inc.) served to quantify particle concentration and determine size distribution of the sEVs [40-42]. Calibration standards included 250 nm SiNPs beads (QS2503, NanoFCM Inc.) for concentration and a Silica Nanosphere Cocktail (S16M-Exo with particles of 68, 91, 113, and 155 nm, NanoFCM Inc.) for sizing. Measurements were based on 1-minute data acquisitions that generated histograms and dot-plots. Dilution in PBS was adjusted to maintain particle detection rates between 3000 and 10000 per minute, with analysis performed at 1.0 kPa pressure. Buffer-only runs provided background controls. The capillary was cleaned with washing buffer (C1801, NanoFCM Inc.) between successive samples. Final analysis relied on NanoFCM Software V1.17 (NanoFCM Inc.).

Total protein

Quantification of total protein in sEVs preparations was achieved with the Pierce BCA Protein Assay Kit (Cat#23225, ThermoFisher) as specified by the manufacturer.

Western blot analysis of protein composition

Cell lysates and sEVs isolates were prepared in RIPA lysis buffer (Beyotime Biotechnology) supplemented with PMSF (10 µL per mL of buffer, Beyotime Biotechnology). After determining protein levels, samples were combined with 5× SDS-PAGE loading buffer (Beyotime Biotechnology) and boiled for 15 min at 95°C. Ten micrograms of protein per lane were separated on 10% SDS-PAGE gels run at 80 V, then transferred to PVDF membranes (Millipore) at 300 mA. Membranes were blocked for 30 min and probed overnight at 4°C in the dark with primary antibodies diluted 1:1000. Antibodies targeted CD9 (ab92726, Abcam), CD63 (ab134045, Abcam), TSG101 (sc-7964, Santa Cruz), Calnexin (2679, Cell Signaling Technology), and GM130 (ab52649, Abcam). Following TBST washes, HRP-linked secondary antibodies were applied for 1 h at room temperature in the dark. Bands were revealed with an enhanced chemiluminescence kit and documented using a Bio-Rad imaging system.

Immunofluorescent staining and single-vesicle protein phenotyping of sEVs

Immunofluorescent labeling of sEVs followed previously published procedures [25, 39-43]. A 100 µL aliquot of sEVs suspension (approximately 1×10^{10} particles/mL) was combined with fluorescein-conjugated antibody and incubated for 60 min at 37°C in the dark. Following incubation, unbound antibodies were removed by diluting the mixture with 1 mL PBS and transferring it to a fresh tube. The sample underwent ultracentrifugation at 100,000 × g for 17 min at 4°C in a Beckman Coulter MAX-XP centrifuge fitted with an MLA-150 rotor. The pellet was redispersed in 1 mL PBS and centrifuged again under identical conditions. After this washing step, the final pellet was resuspended in 50 µL PBS prior to NanoFCM analysis. Bivariate dot-plots of FITC-A versus SS-A were examined in NanoFCM Software V1.17, with linear gating used to separate fluorescein-conjugated antibody-positive sEVs from the unlabeled negative population.

Antibodies utilized in the immunofluorescent staining were: Alexa Fluor 488 (AF488) Mouse Anti-Human CD9 (NanoFCM, NHA009-A488-50T, 1:10), AF488 Mouse Anti-Human CD63 (NanoFCM, NHA063-A488-50T, 1:10), FITC Mouse Anti-Human CD81 (NanoFCM, NHA-FITC-50T, 1:10), Anti-Human CD13 Antibody (EOOXOM, PS04M013F, 1:10), Anti-Human CD29 Antibody (EOOXOM, PS04M029F, 1:10), Anti-Human CD44 Antibody (EOOXOM, PS04M044F, 1:10), Anti-Human CD73 Antibody (EOOXOM, PS04M073F, 1:10), Anti-Human CD90 Antibody (EOOXOM, PS04M090F, 1:10), Anti-Human CD105 Antibody (EOOXOM, PS04M105F, 1:10), AF488 anti-Human CD146 Antibody (BioLegend, 361019, 1:20), AF488 anti-Human CD166 Antibody (ThermoFisher, MA523565, 1:20), AF488 anti-Human CD34 Antibody (BioLegend, 343517, 1:20), FITC Mouse Anti-Human CD45 (BD Pharmingen, 560976, 1:20), and AF488 anti-Human HLA-DR Antibody (BioLegend, 307619, 1:20). Triple staining for CD9/CD63/CD81 involved simultaneous incubation with the respective antibodies at 1:20 each. Triple staining for CD34/CD45/HLA-DR used the corresponding antibodies at 1:50 each.

High-resolution microscopic imaging and computational image analysis

The sEVs were then labeled with the lipophilic membrane dye DiI (Thermo Fisher Scientific, V22885, 1:200) for 30 min at 37°C in the dark. No additional washing was necessary to remove excess DiI, given its low fluorescence intensity when not incorporated into membranes. Ten microliters of the stained sample were applied to an adhesion slide (188105, Citotest) and gently covered with a coverslip. High-resolution fluorescence images were acquired using a 100× oil immersion objective on an IXplore SpinSR10 super-resolution microscope (Olympus).

Image processing and particle analysis were conducted in ImageJ. Signals from fluorescein-conjugated antibodies (marker detection) were assigned green (RGB: 0, 255, 0), while DiI-labeled sEVs were assigned red (RGB: 255, 0, 0) in the microscope output, and merged-channel images were saved. These images were separated into individual color channels and converted to grayscale. The green channel represented marker-specific signals, the red channel corresponded to DiI-stained sEVs, and the blue channel was discarded due to lack of useful data. Grayscale images from the green and red channels underwent smoothing and background subtraction using ImageJ default settings, then were converted to binary format. Particles were detected and enumerated in both channels via the "Analyze Particles" tool with standard parameters. Spots appearing in both channels simultaneously were identified as colocalized and counted separately. The percentage of protein-positive sEVs was determined according to the equation: Positive rate (%) = (Number of colocalized spots / Number of spots in red channel) × 100%.

Assay for sEVs-mediated promotion of cell proliferation

HFF1 cells were seeded into 96-well plates at 2000 cells per well. After 24 h of growth arrest, the cells received treatment with MSC-derived sEVs at a final concentration of 1×10^9 particles/mL in culture medium or an equivalent volume of control medium (MSC-sEVs/PBS mixed with culture medium at a 1:9 ratio, v/v). Cell proliferation was evaluated using the Cell Counting Kit-8 (CCK-8) assay (Dojindo) per the manufacturer's guidelines. On days 0, 1, 2, and 3, 10 μL of CCK-8 solution was added to each well, followed by incubation at 37°C for 1 h. Absorbance readings were taken at 450 nm with a microplate reader (Bio-Rad).

Statistical analysis

All experiments were repeated independently at least three times with biological replicates, and data are reported as mean ± standard deviation (SD). Two-group comparisons were analyzed using Student's t-test, while multiple-group differences were assessed by one-way analysis of variance. All statistical evaluations were performed with GraphPad Prism 9 software.

Results and Discussion

Isolation and characterization of MSC-sEVs

This investigation examined small extracellular vesicles (sEVs) generated by human adipose tissue-derived mesenchymal stem cells (A-MSC-sEVs), human umbilical cord-derived mesenchymal stem cells (U-MSC-sEVs), and induced pluripotent stem cell-derived mesenchymal stem cells (i-MSC-sEVs). Three independent donor-derived cell lines were included for each MSC type. sEVs were harvested from the conditioned medium of the nine MSC lines using differential ultracentrifugation (dUC). Characterization of the resulting MSC-sEVs adhered

to the MISEV2023 standards along with supplementary established criteria [1, 44]. Transmission electron microscopy (TEM) micrographs **(Figure 1a)** confirmed the presence of characteristic cup-shaped morphology in sEVs isolated from all nine cell lines. Analysis by NanoFCM showed that particle size distributions **(Figure 1b)** displayed an asymmetric right-skewed profile with a prominent peak around 80 nm. Average particle diameters for the nine preparations **(Figure 1c)** were largely consistent. However, the quantity of sEVs secreted by the different MSC lines varied considerably, as evidenced by differences in particle **(Figure 1d)** and total protein **(Figure 1e)** concentrations in the conditioned medium. Despite these variations, particle-to-protein ratios for all MSC-sEVs exceeded 1 × 10^8 particles per microgram (μg) of protein **(Figure 1f)**. A-MSC-sEVs specifically yielded ratios of 1.69 ± 0.11, 1.90 ± 0.30, and 1.61 ± 0.34 (× 10^8 particles/μg protein), which were lower compared with U-MSC-sEVs (3.13 ± 0.48, 2.58 ± 0.19, 1.98 ± 0.44 × 10^8 particles/μg protein) and i-MSC-sEVs (3.65 ± 1.11, 3.65 ± 0.52, 4.34 ± 0.31 × 10^8 particles/μg protein). Immunoblotting verified the enrichment of established EV markers CD9, CD63, and TSG101 in every MSC-sEVs sample **(Figure 1g)**, whereas the contaminants GM130 and Calnexin were undetectable **(Figure 1g)**. Overall, these observations established that the isolated vesicles fulfilled essential quality requirements for use in subsequent studies.

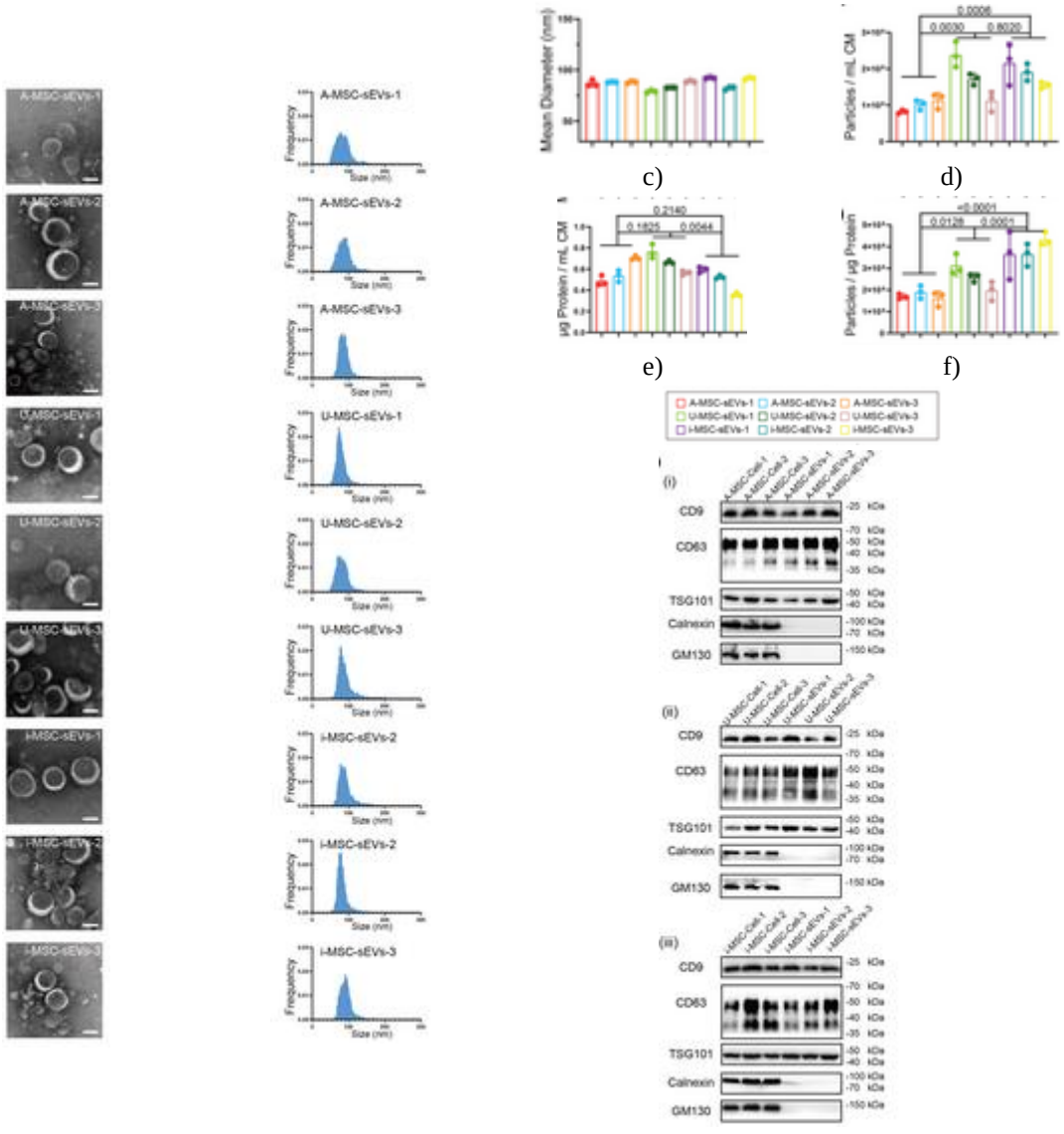

Figure 1. Characterization of small extracellular vesicles obtained from mesenchymal stem cells (MSC-sEVs) generated by nine MSC lines representing three distinct tissue origins.

(a) Transmission electron microscopy images of MSC-sEVs. Scale bar = 100 nm. (B, C) Size distribution profiles (b) and mean diameters (c) of MSC-sEVs as measured by NanoFCM. (d, e) Assessment of sEVs production levels through particle concentration (d) and protein concentration (e) (n = 3). (f) Calculated

particle-to-protein ratios derived from dividing particle counts by protein amounts (n = 3). (g) Western blot results for positive EV markers (CD9, CD63, and TSG101) and negative markers (Calnexin and GM130) in both parent MSCs and purified MSC-sEVs.

Screening for candidate markers of MSC-sEVs through quantitative proteomic analysis

Quantitative proteomics was applied to A-MSC-sEVs, U-MSC-sEVs, and i-MSC-sEVs to identify suitable marker candidates. The protein composition of i-MSC-sEVs was determined directly by liquid chromatography tandem mass spectrometry (LC-MS/MS). Pre-existing quantitative proteomic datasets for A-MSC-sEVs [45] and U-MSC-sEVs [46] were obtained from relevant publications that employed analogous analytical strategies. Parallel proteomic profiling of all three MSC-sEVs types yielded the results summarized in **Figure 2**. A total of 2275 proteins were detected in A-MSC-sEVs, 1149 in U-MSC-sEVs, and 2243 in i-MSC-sEVs, with 87.8%, 96.3%, and 92.2% of these entries respectively matching records in the Vesiclepedia database **(Figure 2a).** The comparatively smaller number of proteins identified in U-MSC-sEVs was likely attributable to differences in mass spectrometry instrumentation and batch-related effects between studies. The top 100 EV proteins, ranked by occurrence frequency in Vesiclepedia datasets, showed strong representation, with 96 of them present in the proteomic profiles of all three MSC-sEVs types **(Figure 2b)**. In keeping with the MISEV2023 five-component framework for EV protein reporting [1], representative proteins and their relative quantities were documented for each MSC-sEVs source. Multiple signature EV proteins, such as CD63, CD81, Alix, Syntenin-1, HSC70, and HSP84, displayed notable enrichment across all samples **(Figure 2c)**. The relative contributions of proteins potentially originating from non-EV structures, non-plasma membrane/endosomal compartments, and secreted factors are illustrated in **Figure 2d**. Extracellular matrix constituents (e.g., FN1, COL6A3, COL1A1, and MFGE8) were among the most abundant components, while cytokines, growth factors, and unrelated non-membrane proteins occurred at minimal levels or were absent. These proteomic patterns indicated a high degree of similarity in EV protein composition among the three MSC sources and validated the datasets for downstream marker screening.

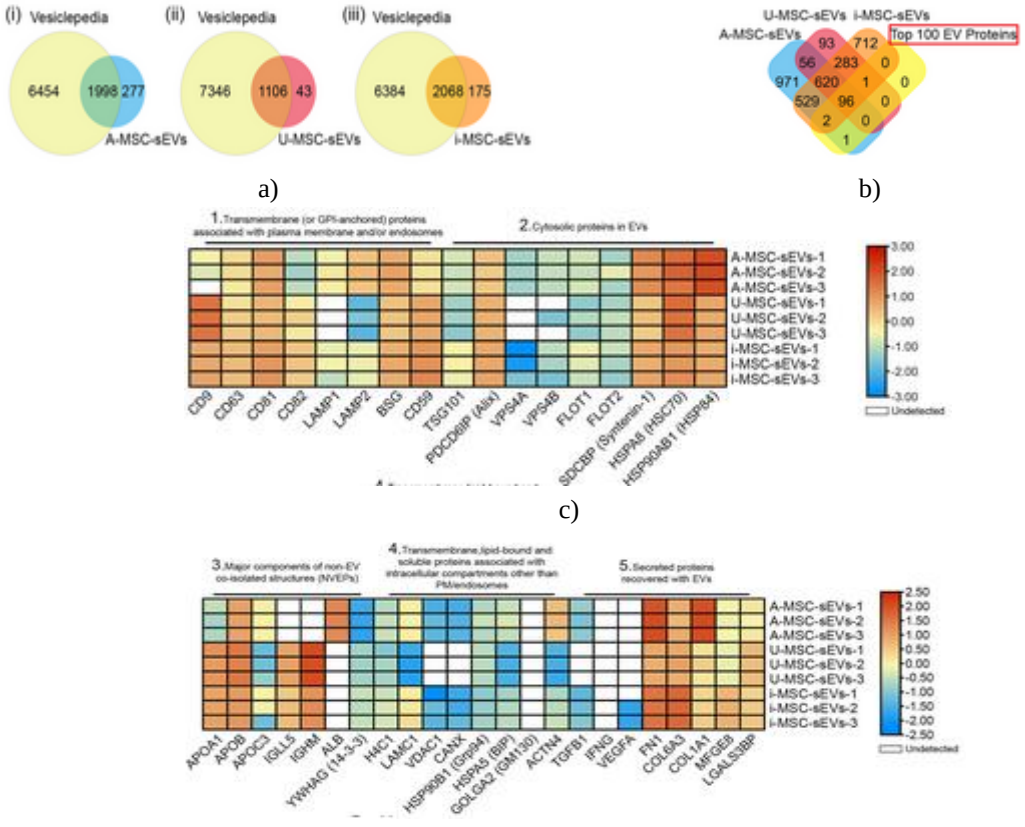

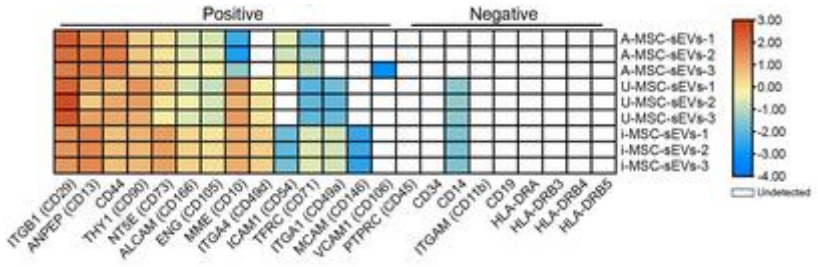

e)

Figure 2. Proteomic characterization of mesenchymal stem cell-derived small extracellular vesicles (MSC-sEVs). Liquid chromatography tandem mass spectrometry (LC-MS/MS) followed by bioinformatics processing was utilized to catalog protein constituents within MSC-sEVs.
(a) Venn diagram depicting shared and unique proteins identified in A-MSC-sEVs, U-MSC-sEVs, and i-MSC-sEVs in relation to the Vesiclepedia database. (b) Venn diagram highlighting the overlap of the top 100 EV proteins with those detected in MSC-sEVs. (C–E) Heatmaps based on corrected Log2 label-free quantification (LFQ) intensity displaying the five-component EV protein framework (c, d) and selected MSC-associated membrane proteins (e) across the MSC-sEVs proteomic datasets (n = 3).

Standard MSC surface antigens documented in the proteomic datasets—such as CD73(+), CD90(+), CD105(+), CD10(+), CD13(+), CD29(+), CD44(+), CD49a(+), CD49d(+), CD54(+), CD71(+), CD106(+), CD146(+), CD166(+), CD45(−), CD34(−), CD14(−), CD11b(−), CD19(−), and HLA-DR(−) [26-30]—were specifically evaluated. Their expression levels in A-MSC-sEVs, U-MSC-sEVs, and i-MSC-sEVs are shown in **Figure 2e**. Proteins CD29, CD13, CD44, CD90, CD73, CD166, and CD105 were abundantly represented in sEVs from all three MSC origins. Conversely, negative markers (CD45, CD34, CD14, CD11b, CD19, and HLA-DR) appeared at trace levels or were completely absent. Accordingly, CD29, CD13, CD44, CD90, CD73, CD166, and CD105 were advanced as promising candidate markers for further examination in these MSC-sEVs populations.

Identification of MSC-sEVs markers at single-vesicle resolution

Single-vesicle flow cytometry via NanoFCM was utilized to determine the exact proportion of vesicles expressing each candidate surface marker. The analysis encompassed the selected MSC-sEVs candidates (CD13, CD29, CD44, CD73, CD90, CD105, and CD166) along with three broadly recognized EV markers (CD9, CD63, and CD81). CD146, noted for its limited presence in the proteomic survey, was additionally examined to confirm consistency with LC-MS/MS results. Samples were processed through immunofluorescence labeling followed by removal of free antibodies prior to NanoFCM measurement **(Figure 3)**. Positivity for CD9 displayed notable variation among sEVs from the nine MSC lines representing the three sources **(Figure 3a)**. CD63 positivity remained relatively stable near 50% across all preparations **(Figure 3b)**. CD81 achieved a substantially higher average positivity rate of 66.9 ± 3.8% **(Figure 3c)**. Triple labeling for the CD9/CD63/CD81 combination yielded consistent positivity approaching 80% in the MSC-sEVs population **(Figure 3d)**.

Regarding the candidate markers, CD13 maintained strong positivity exceeding 70% in sEVs from every MSC line, averaging 83.2 ± 5.1% **(Figure 3e)**. CD29 and CD90 likewise showed reliable detection above 60% in all nine lines, with mean values of 74.1 ± 5.5% and 70.3 ± 4.4% **(Figures 3f and 3i)**. CD44 positivity fluctuated more widely between 23.0% and 53.1% **(Figure 3g)**. Conversely, CD73 **(Figure 3h)**, CD105 **(Figure 3j)**, CD146 **(Figure 3k)**, and CD166 **(Figure 3l)** registered positivity rates under 30%. Combined assessment of negative MSC markers revealed negligible signals across the tested sEVs. CD34, frequently expressed by several cell populations that commonly share the MSC microenvironment (e.g., fibroblasts, preadipocytes, endothelial cells, and hematopoietic stem cells [47-51]), was undetectable in MSCs and their sEVs from all sources, indicating its value as an exclusion marker. Overall, CD13, CD29, and CD90 stood out with consistently high positivity rates above 60% in sEVs derived from the three MSC types **(Figure 3m),** highlighting their potential as characteristic markers.

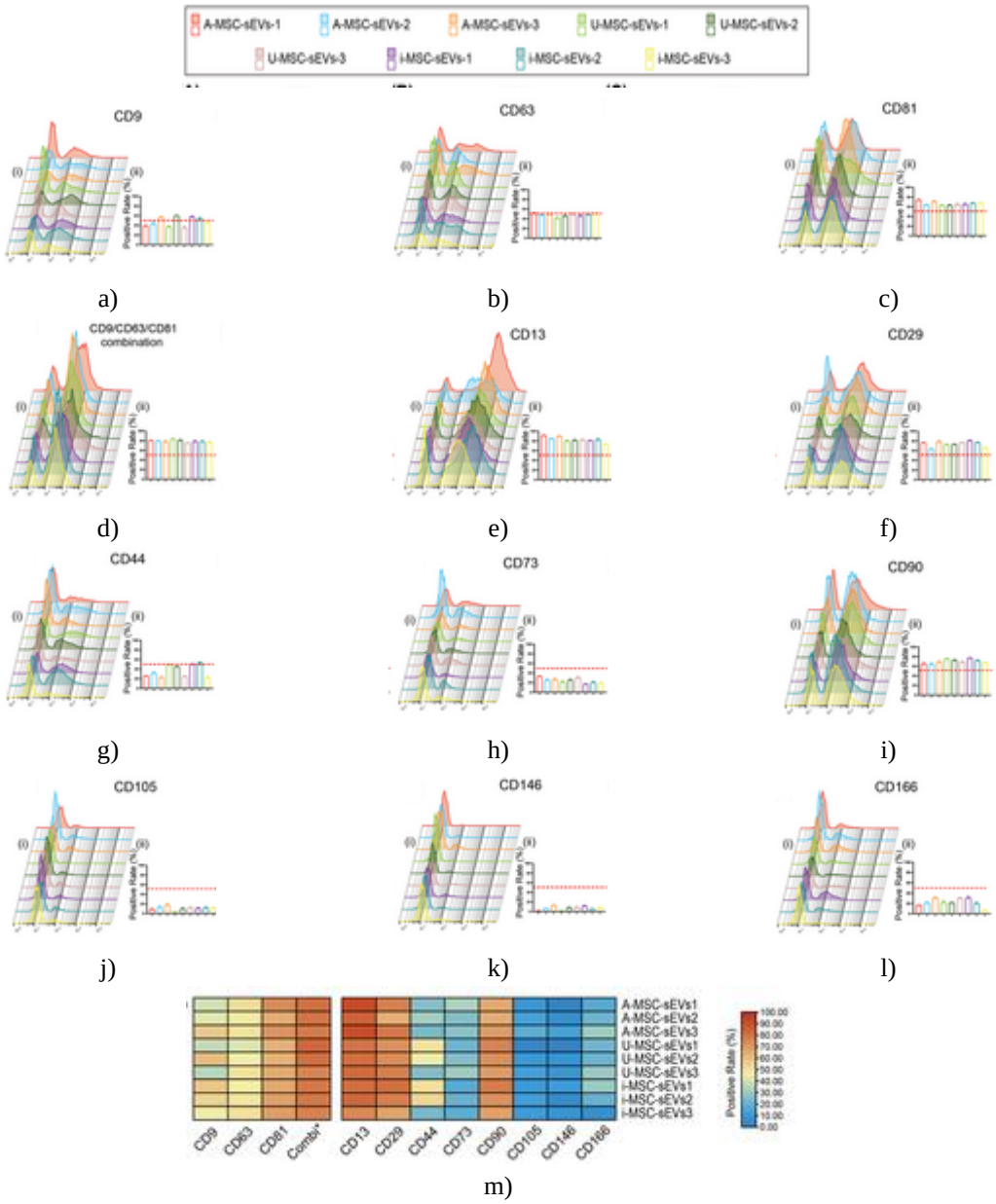

Figure 3. Detection of potential markers on mesenchymal stem cell-derived small extracellular vesicles (MSC-sEVs) using single-vesicle resolution techniques. (a–d) NanoFCM results for common EV markers CD9 (a), CD63 (b), CD81 (c), and the CD9/CD63/CD81 triple combination (d). (e–l) NanoFCM results for candidate MSC-sEVs markers CD13 (e), CD29 (f), CD44 (g), CD73 (h), CD90 (i), CD105 (j), CD146 (k), and CD166 (l). Left panels (i) display fluorescence intensity histograms; right panels (ii) present bar graphs of positivity rates across nine MSC-sEVs lines (n = 3). (M) Heatmap illustrating average positivity rates for each marker in the nine MSC-sEVs preparations (n = 3). Combi, CD9/CD63/CD81 combination.

Validation of candidate markers in MSC-sEVs obtained by DGUC and SEC

To account for possible differences in protein profiles arising from alternative purification strategies [1, 52], MSC-sEVs were additionally isolated using sucrose density gradient ultracentrifugation (DGUC) and size exclusion chromatography (SEC) **(Figure 4a)**. Fractions from both methods were evaluated for particle concentration, protein content, and particle-to-protein ratios **(Figures 4b and 4c)**. The top three fractions demonstrating superior particle enrichment and optimal ratios were selected for NanoFCM testing. Positivity rates observed for universal EV markers (CD9, CD63, CD81) and candidate MSC markers (CD13, CD29, CD90) in DGUC- and SEC-derived sEVs closely matched those from dUC isolation **(Figures 4d–4j)**. These outcomes reinforced that CD13, CD29, and CD90 function as robust and consistently abundant markers irrespective of the isolation technique applied.

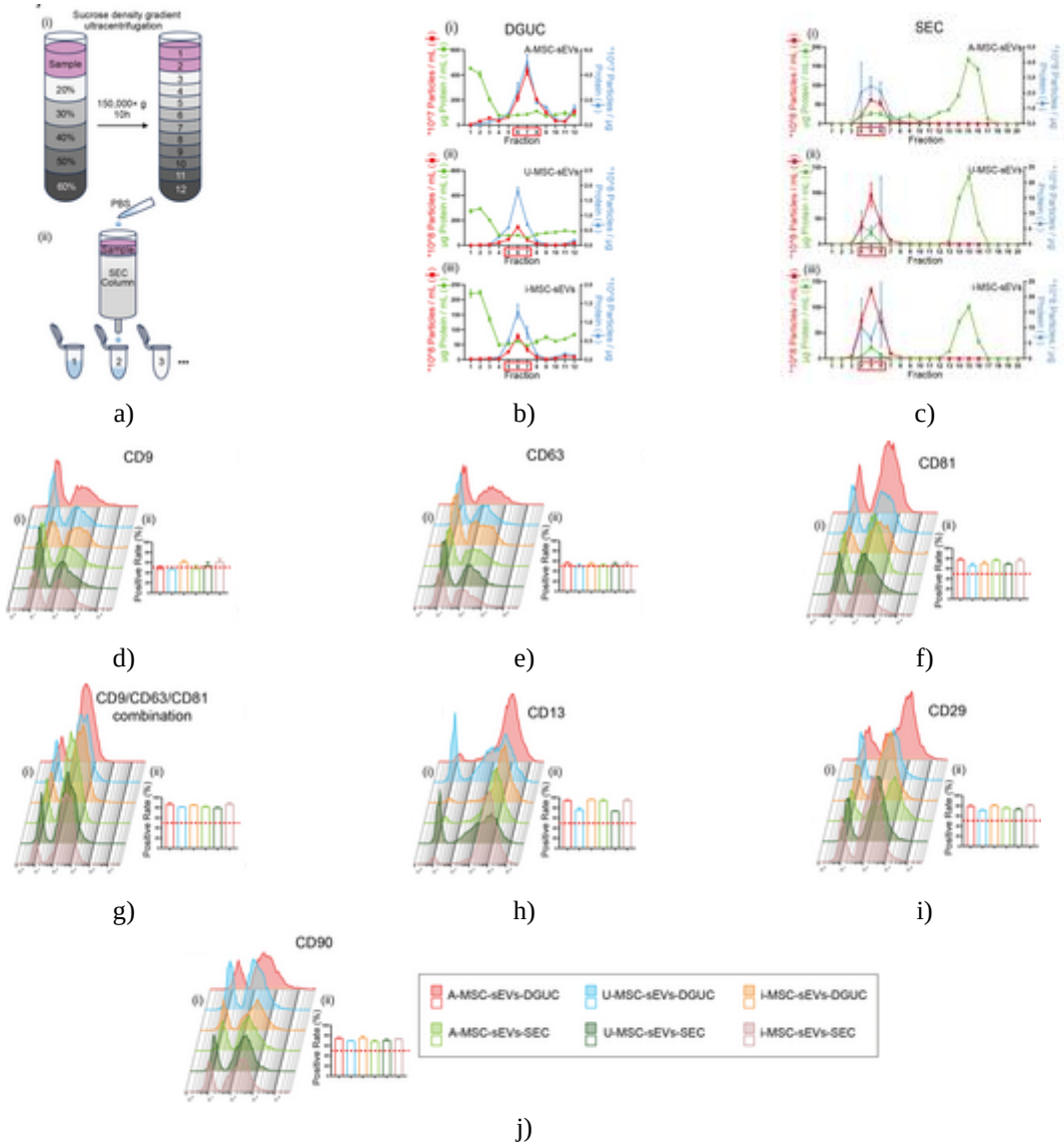

Figure 4. NanoFCM evaluation of candidate markers in nine lines of mesenchymal stem cell-derived small extracellular vesicles (MSC-sEVs) purified via density gradient ultracentrifugation (DGUC) and size exclusion chromatography (SEC). (a) Procedural overview for DGUC and SEC isolation. (b, c) Profiles of particle concentration, protein concentration, and particle-to-protein ratios for fractions collected through DGUC (b) and SEC (c) (n = 3). sEVs-enriched fractions are indicated by red rectangles. (d–j) NanoFCM data for selected markers. Left panels (i) show fluorescence histograms; right panels (ii) display bar graphs of positivity rates (n = 3).

High-resolution microscopic imaging of candidate markers on MSC-sEVs

An orthogonal validation approach employing high-resolution fluorescence microscopy was adopted to reduce method-specific bias [41, 53] and directly visualize universal EV markers (CD9, CD63, CD81) as well as candidate MSC-sEVs markers (CD13, CD29, CD90). sEVs were initially labeled with green fluorescein-conjugated antibodies targeting the respective proteins. Excess antibodies were removed, after which vesicles were stained with the lipophilic dye DiI and examined by super-resolution microscopy **(Figure 5a)**. Computational image analysis was subsequently applied to count DiI-positive (purple) spots representing sEVs, green marker signals, and overlapping colocalized events **(Figure 5b)**. Positive rates were expressed as the percentage of colocalized spots among total DiI-labeled vesicles. Microscopy-based quantification **(Figure 5c)** produced results comparable to NanoFCM data: CD9 (63.4 ± 5.8%), CD63 (54.3 ± 4.0%), CD81 (70.9 ± 2.3%), and the CD9/CD63/CD81 combination (76.8 ± 2.5%). The candidate markers similarly demonstrated strong performance with CD13 at 74.0 ± 9.4%, CD29 at 73.7 ± 4.0%, and CD90 at 73.2 ± 6.5%. These independent

single-vesicle imaging results provide further confirmation that CD13, CD29, and CD90 serve as reliable markers for MSC-derived sEVs.

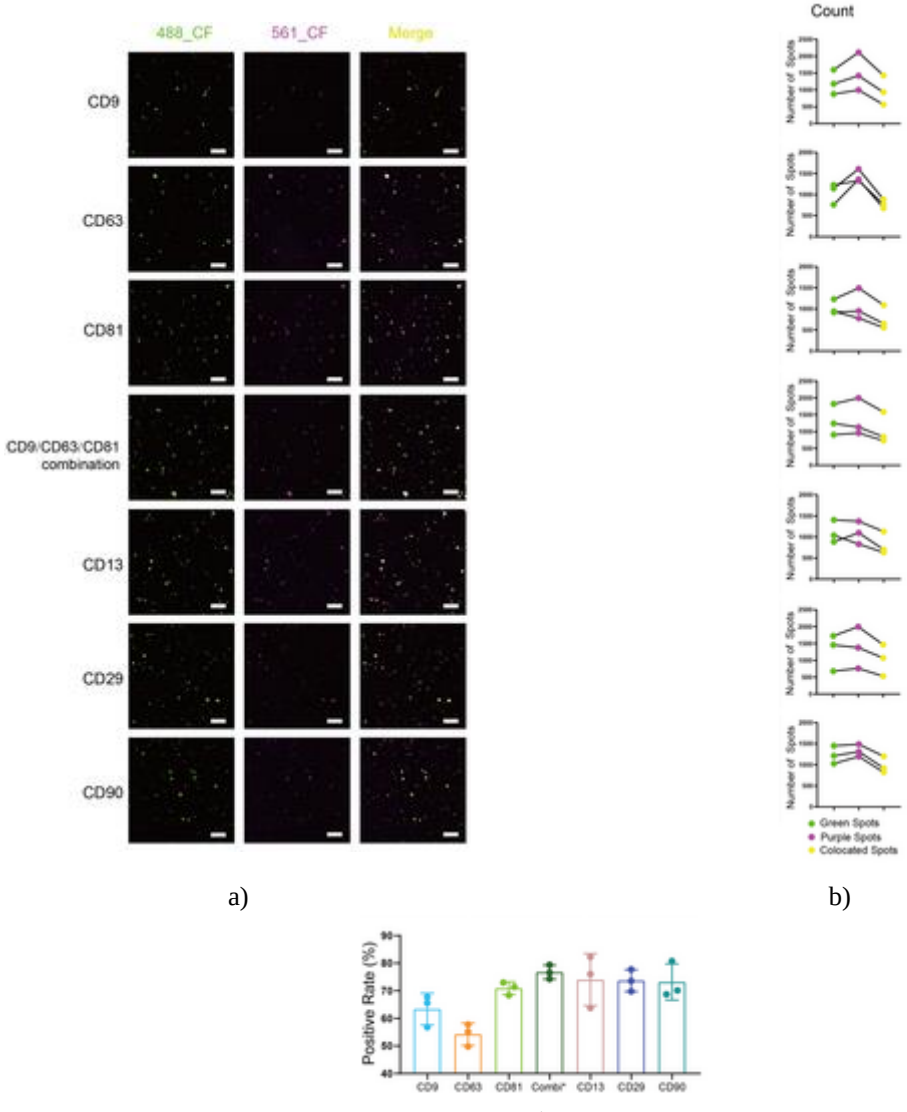

Figure 5. High-resolution imaging-based quantification of candidate markers present on mesenchymal stem cell-derived small extracellular vesicles (MSC-sEVs). (a) Representative super-resolution micrographs of A-MSC-sEVs stained with DiI (561_CF) and fluorescein-conjugated antibodies specific for the indicated markers (488_CF). Scale bar = 5 µm. (b) Enumeration of purple (sEVs), green (marker), and colocalized spots per image. Connected data points correspond to measurements from the same image. (c) Calculated positive rates based on the fraction of colocalized spots relative to DiI-positive vesicles (n = 3). Combi, CD9/CD63/CD81 combination.

Specificity of the candidate MSC-sEVs markers

Specificity of the proposed markers was examined by performing detailed NanoFCM profiling on sEVs generated from six distinct non-MSC cell lines. These included vesicles isolated via differential ultracentrifugation from HFF1, 293T, A549, H460, MCF7, and MDA-MB-231 cells, all of which were subjected to standard characterization. Direct comparison of marker positivity was conducted between the nine MSC-sEVs lines and the six non-MSC sEVs samples for both common EV markers (CD9, CD63, CD81) and the candidate MSC markers (CD13, CD29, CD90) **(Figure 6)**. In MSC-derived vesicles, positivity for the candidate markers remained above 60% in every case. By comparison, non-MSC sEVs failed to show simultaneous positivity above 40% for this set of markers **(Figures 6a–6d)**. Universal EV markers such as CD9 and CD63, along with the

CD9/CD63/CD81 triple combination, offered limited discriminatory power between the two groups. Only CD81 displayed noticeably higher positivity within MSC-sEVs **(Figures 6e–6i)**. The data therefore establish CD13, CD29, and CD90 as highly specific identifiers of MSC-sEVs when analyzed at single-vesicle resolution. Application of a 50% positivity threshold across all three markers enables reliable differentiation of MSC-sEVs from vesicles originating from non-MSC sources.

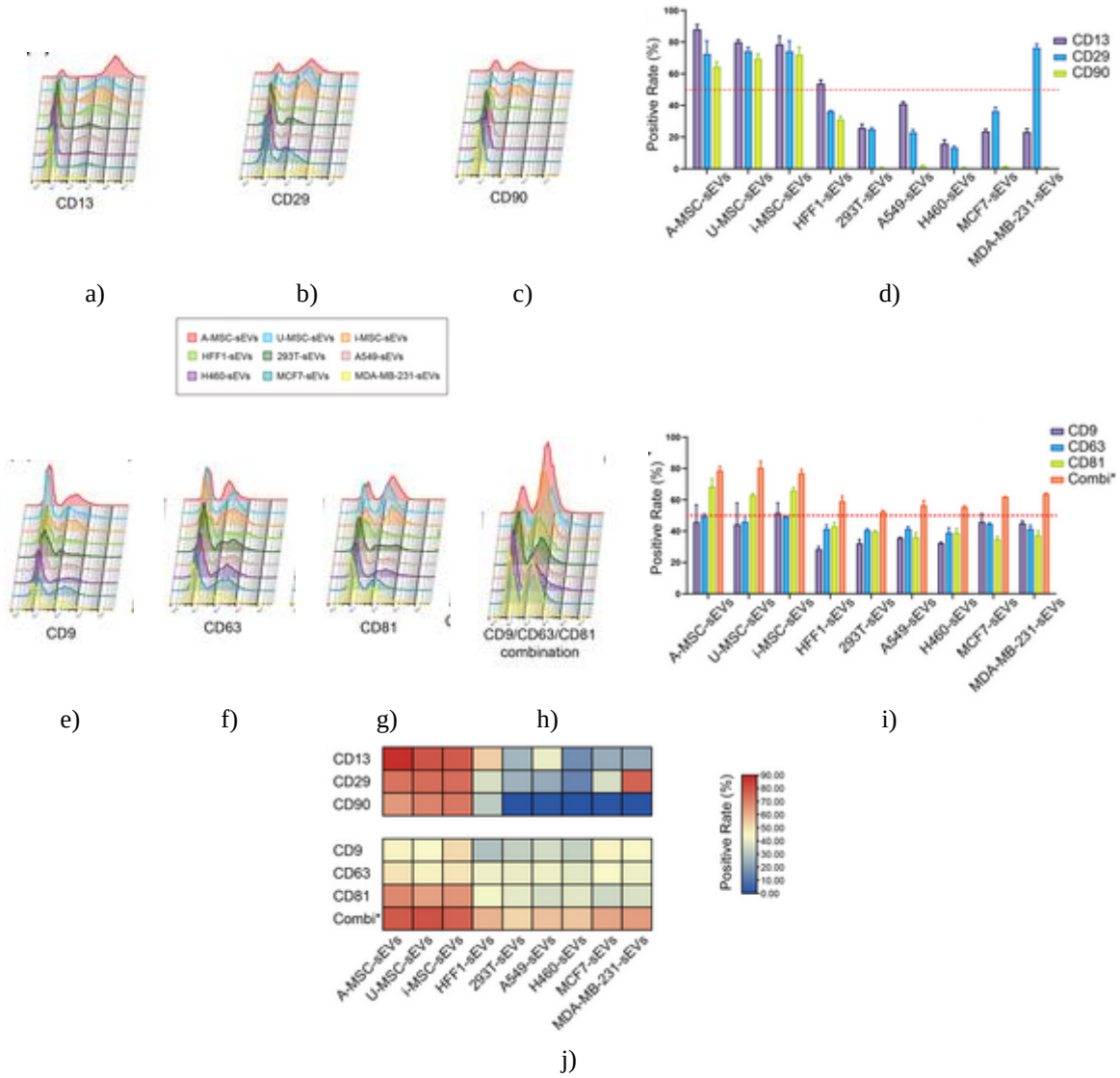

Figure 6. Evaluation of specificity for candidate markers associated with mesenchymal stem cell-derived small extracellular vesicles (MSC-sEVs). Validation involved sEVs prepared from six non-MSC cell lines. (a–c) NanoFCM-based surface phenotyping of candidate markers CD13 (A), CD29 (b), and CD90 (c) on vesicles from MSC and non-MSC origins. (d) Compiled positivity rates for the candidate MSC-sEVs markers (n = 3). (e–h) NanoFCM phenotyping of universal EV markers CD9 (e), CD63 (f), CD81 (g), and the CD9/CD63/CD81 triple combination (h) across the complete set of sEVs. (i) Summary of positivity rates for universal EV markers (n = 3). (j) Heatmap summarizing average positivity for each marker across all sEVs examined (n = 3). Combi, CD9/CD63/CD81 combination.

Association between the marker panel and functional performance of MSC-sEVs

The practical significance of the marker panel was further explored by examining its relationship to the biological activity of MSC-sEVs. Vesicles were harvested from MSCs cultured through passages 5, 7, 10, and 12, and their ability to enhance fibroblast (HFF1) proliferation was tested via CCK-8 assay. Progressive loss of proliferative stimulation was evident with advancing passage number **(Figure 7a)**, consistent with declining functional capacity of MSC-sEVs over extended culture. Surface marker expression on the parent MSCs for CD13, CD29, CD44,

CD73, CD90, and CD105 showed only minor fluctuations across these passages. However, when assessed on the released sEVs, positivity for CD29 and CD90 exhibited a clear downward trend, dropping beneath 50% by passage 12, while CD13 positivity persisted at approximately 80% **(Figures 7b and 7c)**. These results imply that declining positivity for CD29 and CD90 in sEVs may reliably indicate reduced functional quality.

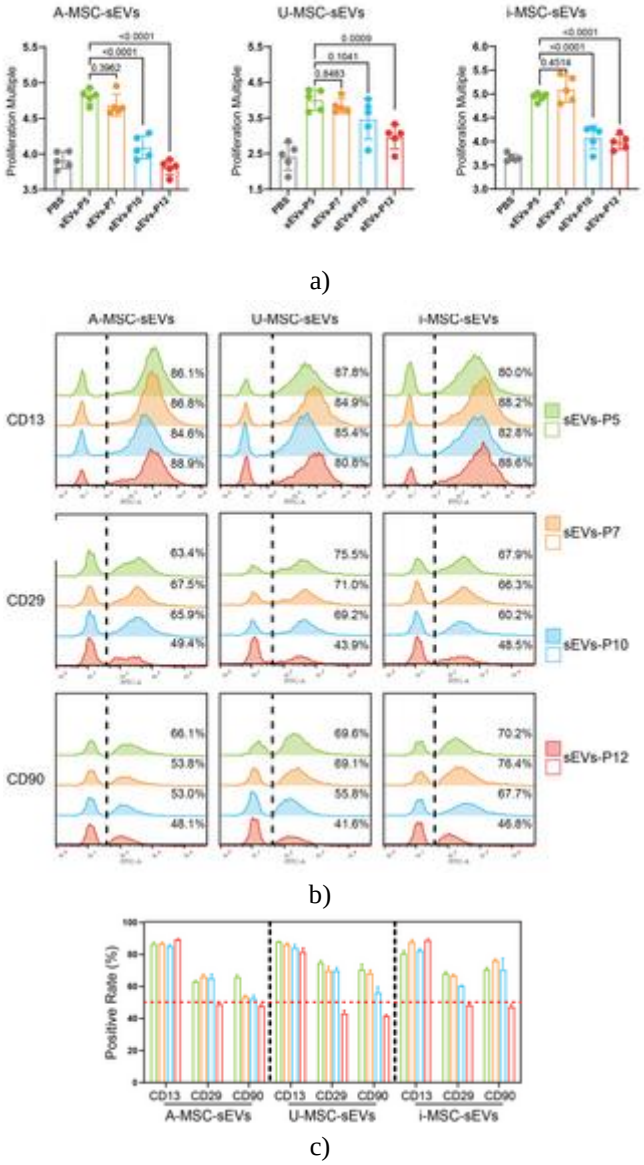

Figure 7. Link between the marker panel and functional characteristics of mesenchymal stem cell-derived small extracellular vesicles (MSC-sEVs). sEVs were collected from MSCs maintained at passages 5, 7, 10, and 12. (a) Proliferation fold-change in HFF1 cells following exposure to sEVs from MSCs at increasing passages, determined by CCK-8 measurement on day 3 (n = 5). (b) NanoFCM surface phenotyping of the marker panel (CD13, CD29, and CD90) on sEVs released by MSCs at successive passages. (c) Positivity rates recorded for CD13, CD29, and CD90 in sEVs from MSCs at different passage numbers (n = 3).

Mesenchymal stromal cell-derived small extracellular vesicles (MSC-sEVs) have attracted growing attention as candidate therapeutic agents and are now being assessed in multiple clinical trials [21, 22]. Nevertheless, universally accepted standards for defining and qualifying human MSC-sEVs preparations are still absent [21, 24]. The unavailability of reliable, quantifiable, and selective markers for these preparations has complicated data exchange and cross-comparison of batches produced independently, thereby delaying their successful clinical development. The current study employed detailed NanoFCM profiling and, for the first time, demonstrated that MSC-sEVs isolated from three different sources—adipose tissue, umbilical cord, and induced pluripotent stem

cells—exhibited positive rates for CD13, CD29, and CD90 that consistently surpassed 60% when analyzed at the single-vesicle level. In addition, the study confirmed the specificity of this protein combination, showing that the panel consisting of CD13, CD29, and CD90 could effectively separate MSC-sEVs from vesicles derived from non-MSC cells. Moreover, a clear positive association was established between the functional potency of MSC-sEVs and the surface positivity for CD29 and CD90. These observations support the proposal of CD13, CD29, and CD90 as a distinctive marker panel for MSC-sEVs generated from the three examined sources.

To account for source-related heterogeneity, the investigation included adipose-derived MSCs (A-MSCs), umbilical cord-derived MSCs (U-MSCs), and iPSC-derived MSCs (i-MSCs) in order to pinpoint shared surface markers on the secreted sEVs. Both A-MSCs and U-MSCs can be readily obtained from routine medical by-products, representing an abundant and practical resource [35, 36]. iPSCs, with their extensive self-renewal capacity and potential for indefinite expansion, enable ongoing generation of i-MSCs and are therefore well suited for scaled-up manufacturing of MSC-sEVs [54, 55]. By thoroughly characterizing the surface proteome and phenotype of sEVs released by these three MSC types, the study uncovered a consistent group of highly expressed markers common to all. Earlier proteomic work by Van Balkom *et al*. examined published EV datasets from MSCs of several origins, including placenta, bone marrow, umbilical cord, adipose tissue, and embryonic stem cells, although coverage of the sources was not uniform [31]. Similarly, Nguyen *et al*. analyzed eleven MSC-sEVs preparations originating from five independent laboratories that varied in cell source, culture parameters, and isolation procedures [56]. Unlike many prior reports that focused on a single MSC type or origin [32–34], incorporating vesicles from multiple sources enhanced the robustness and broader applicability of the marker validation. As expected, some variation in candidate marker positivity was observed across the different MSC-sEV populations.

Adequate definition of MSC-sEVs preparations depends not only on suitable markers but also on the availability of reproducible, standardized measurement techniques [24]. In previous decades, researchers have relied on a range of qualitative or semi-quantitative approaches to evaluate MSC-sEVs surface markers. For example, Munshi *et al*. captured sEVs from bone marrow-derived MSCs using CD63-coated beads and profiled 37 reported human CD antigens, revealing stronger signals for CD81, CD29, CD44, CD105, CD146, and MCSP relative to CD63 [33]. In contrast, Jakl *et al*., employing a comparable bead-based flow cytometry strategy, noted reduced expression of CD81, CD44, and CD105 compared with CD63 on B-MSC-derived sEVs [52]. Nguyen *et al*. extended such testing across eleven preparations that differed in origin, culture, and isolation methods, designating CD44, CD73, and CD105 as positive and CD11b, CD45, and CD197 as negative markers [56]. Wiklander *et al*. pointed out that bead-based assays are highly sensitive to the choice of tetraspanin-targeted capture reagents (such as CD9, CD63, or CD81), which may underlie contradictory findings in the literature [34]. These methods lack single-vesicle resolution, cannot accurately quantify the fraction of marker-positive vesicles, and are influenced by immobilization conditions on beads, limiting their utility for standardized quantitative work. The present study therefore utilized NanoFCM, which provides true single-vesicle resolution without requiring vesicle immobilization, to determine the proportion of MSC-sEVs expressing each marker [41]. This approach confirmed that CD13, CD29, and CD90 positivity remained above 60% across sEVs from diverse MSC sources. In comparison, CD44 positivity showed marked source-dependent variability among nine MSC lines, and positivity for CD73, CD105, CD146, and CD166 stayed below 30%. Consequently, CD13, CD29, and CD90 emerged as superior marker candidates. To exclude bias introduced by isolation procedures, MSC-sEVs prepared by differential ultracentrifugation (dUC), density gradient ultracentrifugation (DGUC), and size-exclusion chromatography (SEC) were tested; positivity for the three selected markers stayed consistently above 60% regardless of the method. Orthogonal confirmation was obtained through high-resolution imaging, which visually corroborated the NanoFCM results. Collectively, these lines of evidence establish CD13, CD29, and CD90 as robust and reliable markers for MSC-sEVs.

Verifying the discriminatory power of the proposed panel represents another critical requirement. Many surface antigens, including CD13, CD29, CD44, CD73, CD90, and CD105, are expressed across numerous cell lineages [26–30]. A single antigen is therefore insufficient for specific identification of MSCs or their vesicles, and combinations are routinely used. Earlier investigations had not clarified which antigens best separate MSC-sEVs from non-MSC-derived vesicles. Here, positivity for CD13, CD29, and CD90 was quantified in MSC-sEVs from the three sources and benchmarked against sEVs from six non-MSC cell lines. Individual markers alone failed to provide clear separation. For instance, HFF1-sEVs displayed 53.8 ± 2.3% CD13 positivity, and MDA-MB-231-sEVs reached 76.5 ± 2.2% CD29 positivity, values overlapping with MSC-sEV profiles **(Figure 6)**. Importantly,

MSC-sEVs consistently showed >60% positivity for each of the three markers, whereas non-MSC-sEVs rarely exceeded 40% positivity for all three simultaneously. These data indicate that requiring >50% positivity for CD13, CD29, and CD90 together at the single-vesicle level offers a specific criterion for distinguishing MSC-sEVs.

The study also explored the relationship between marker expression and vesicle function. Progressive passaging of MSCs, which leads to replicative senescence, was accompanied by a gradual decline in the biological activity of derived sEVs, particularly their capacity to stimulate cell proliferation. This functional deterioration coincided with decreasing positivity for CD29 and CD90, while CD13 levels remained largely unchanged. The positive correlation between CD29/CD90 expression and sEV functionality suggests that quantitative single-vesicle measurement of these two markers can serve as a practical surrogate for quality control. Such an approach provides a straightforward, scalable method for monitoring MSC-sEVs during large-scale production and clinical application, supporting their standardization as therapeutic products.

Conclusion

Overall, MSC-sEVs have demonstrated consistent immunomodulatory and tissue-regenerative effects, prompting substantial clinical interest [32, 33]. A growing number of registered trials are now investigating their therapeutic performance [21, 22]. This work establishes CD13, CD29, and CD90 as a specific marker panel applicable to A-MSC-sEVs, U-MSC-sEVs, and i-MSC-sEVs. Implementation of this panel will facilitate the creation of quantifiable, reproducible assays for both identification and quality assurance of MSC-sEVs preparations. These improvements should promote better comparability and data integration across independently generated batches. To increase robustness and translational impact, future studies should expand testing to MSCs from additional tissue origins, donor backgrounds, and disease contexts; examine vesicles produced under varied culture and manufacturing conditions; and further validate the marker panel. Parallel functional evaluations of MSC-sEVs—assessing effects on cell proliferation, migration, apoptosis suppression, and inflammation modulation—will also be necessary. Ongoing research and scientific dialogue are required to define reliable functional assays tailored to different clinical indications. The development of consensus-based standardized criteria for MSC-sEVs will significantly accelerate their safe and effective translation into clinical therapies.

Acknowledgments: None

Conflict of Interest: None

Financial Support: None

Ethics Statement: None

References

1. Welsh JA, Goberdhan DCI, O'Driscoll L, Buzas EI, Blenkiron C, Bussolati B, et al. Minimal information for studies of extracellular vesicles (MISEV2023): from basic to advanced approaches. J Extracell Vesicles. 2024;13(2):e12404. doi:10.1002/jev2.12404
2. Colombo M, Raposo G, Théry C. Biogenesis, secretion, and intercellular interactions of exosomes and other extracellular vesicles. Annu Rev Cell Dev Biol. 2014;30:255-89. doi:10.1146/annurev-cellbio-101512-122326
3. Valadi H, Ekström K, Bossios A, Sjöstrand M, Lee JJ, Lötvall JO. Exosome-mediated transfer of mRNAs and microRNAs is a novel mechanism of genetic exchange between cells. Nat Cell Biol. 2007;9(6):654-9. doi:10.1038/ncb1596
4. Théry C, Ostrowski M, Segura E. Membrane vesicles as conveyors of immune responses. Nat Rev Immunol. 2009;9(8):581-93. doi:10.1038/nri2567
5. van Niel G, D'Angelo G, Raposo G. Shedding light on the cell biology of extracellular vesicles. Nat Rev Mol Cell Biol. 2018;19(4):213-28. doi:10.1038/nrm.2017.125
6. Kalluri R, LeBleu VS. The biology, function, and biomedical applications of exosomes. Science. 2020;367(6478):eaau6977. doi:10.1126/science.aau6977

7. Zhang J, Guan J, Niu X, Hu G, Guo S, Li Q, et al. Exosomes released from human induced pluripotent stem cells-derived MSCs facilitate cutaneous wound healing by promoting collagen synthesis and angiogenesis. J Transl Med. 2015;13:49. doi:10.1186/s12967-015-0417-0
8. Hu GW, Li Q, Niu X, Hu B, Liu J, Zhou SM, et al. Exosomes secreted by human-induced pluripotent stem cell-derived mesenchymal stem cells attenuate limb ischemia by promoting angiogenesis in mice. Stem Cell Res Ther. 2015;6(1):10. doi:10.1186/scrt546
9. Qi X, Zhang J, Yuan H, Xu Z, Li Q, Niu X, et al. Exosomes secreted by human-induced pluripotent stem cell-derived mesenchymal stem cells repair critical-sized bone defects through enhanced angiogenesis and osteogenesis in osteoporotic rats. Int J Biol Sci. 2016;12(7):836-49. doi:10.7150/ijbs.14809
10. Nassar W, El-Ansary M, Sabry D, Mostafa MA, Fayad T, Kotb E, et al. Umbilical cord mesenchymal stem cells derived extracellular vesicles can safely ameliorate the progression of chronic kidney diseases. Biomater Res. 2016;20:21. doi:10.1186/s40824-016-0068-0
11. Wang B, Yao K, Huuskes BM, Shen HH, Zhuang J, Godson C, et al. Mesenchymal stem cells deliver exogenous microRNA-let7c via exosomes to attenuate renal fibrosis. Mol Ther. 2016;24(7):1290-301. doi:10.1038/mt.2016.90
12. Gong ZT, Xiong YY, Ning Y, Tang RJ, Xu JY, Jiang WY, et al. Nicorandil-pretreated mesenchymal stem cell-derived exosomes facilitate cardiac repair after myocardial infarction via promoting macrophage M2 polarization by targeting miR-125a-5p/TRAF6/IRF5 signaling pathway. Int J Nanomedicine. 2024;19:2005-24. doi:10.2147/IJN.S441307
13. Lu Y, Zhang J, Han B, Yu Y, Zhao W, Wu T, et al. Extracellular vesicles DJ-1 derived from hypoxia-conditioned hMSCs alleviate cardiac hypertrophy by suppressing mitochondria dysfunction and preventing ATRAP degradation. Pharmacol Res. 2023;187:106607. doi:10.1016/j.phrs.2022.106607
14. Xie Y, Sun Y, Liu Y, Zhao J, Liu Q, Xu J, et al. Targeted delivery of RGD-CD146+CD271+ human umbilical cord mesenchymal stem cell-derived exosomes promotes blood-spinal cord barrier repair after spinal cord injury. ACS Nano. 2023;17(18):18008-24. doi:10.1021/acsnano.3c04423
15. Xie X, Song Q, Dai C, Cui S, Tang R, Li S, et al. Clinical safety and efficacy of allogenic human adipose mesenchymal stromal cells-derived exosomes in patients with mild to moderate Alzheimer's disease: a phase I/II clinical trial. Gen Psychiatr. 2023;36(5):e101143. doi:10.1136/gpsych-2023-101143
16. Yang W, Pan Z, Zhang J, Wang L, Lai J, Zhou S, et al. Extracellular vesicles from adipose stem cells ameliorate allergic rhinitis in mice by immunomodulatory. Front Immunol. 2023;14:1302336. doi:10.3389/fimmu.2023.1302336
17. Sengupta V, Sengupta S, Lazo A, Woods P, Nolan A, Bremer N. Exosomes derived from bone marrow mesenchymal stem cells as treatment for severe COVID-19. Stem Cells Dev. 2020;29(12):747-54. doi:10.1089/scd.2020.0080
18. Keshtkar S, Azarpira N, Ghahremani MH. Mesenchymal stem cell-derived extracellular vesicles: novel frontiers in regenerative medicine. Stem Cell Res Ther. 2018;9(1):63. doi:10.1186/s13287-018-0791-7
19. Rani S, Ryan AE, Griffin MD, Ritter T. Mesenchymal stem cell-derived extracellular vesicles: toward cell-free therapeutic applications. Mol Ther. 2015;23(5):812-23. doi:10.1038/mt.2015.44
20. Elsharkasy OM, Nordin JZ, Hagey DW, de Jong OG, Schiffelers RM, EL Andaloussi S, et al. Extracellular vesicles as drug delivery systems: why and how? Adv Drug Deliv Rev. 2020;159:332-43. doi:10.1016/j.addr.2020.04.004
21. Kosanović M, Milutinović B, Kutzner TJ, Mouloud Y, Bozic M. Clinical prospect of mesenchymal stromal/stem cell-derived extracellular vesicles in kidney disease: challenges and the way forward. Pharmaceutics. 2023;15(7):1911. doi:10.3390/pharmaceutics15071911
22. Börger V, Bremer M, Ferrer-Tur R, Gockeln L, Stambouli O, Becic A, et al. Mesenchymal stem/stromal cell-derived extracellular vesicles and their potential as novel immunomodulatory therapeutic agents. Int J Mol Sci. 2017;18(7):1450. doi:10.3390/ijms18071450
23. Li M, Huang H, Wei X, Li H, Li J, Xie B, et al. Clinical investigation on nebulized human umbilical cord MSC-derived extracellular vesicles for pulmonary fibrosis treatment. Signal Transduct Target Ther. 2025;10:179. doi:10.1038/s41392-025-02227-7
24. Witwer KW, Van Balkom BWM, Bruno S, Choo A, Dominici M, Gimona M, et al. Defining mesenchymal stromal cell (MSC)-derived small extracellular vesicles for therapeutic applications. J Extracell Vesicles. 2019;8(1):1609206. doi:10.1080/20013078.2019.1609206

25. Chen Z, Luo L, Ye T, Zhou J, Niu X, Yuan J, et al. Identification of specific markers for human pluripotent stem cell-derived small extracellular vesicles. J Extracell Vesicles. 2024;13(2):e12409. doi:10.1002/jev2.12409
26. Dominici M, Le Blanc K, Mueller I, Slaper-Cortenbach I, Marini FC, Krause DS, et al. Minimal criteria for defining multipotent mesenchymal stromal cells. The International Society for Cellular Therapy position statement. Cytotherapy. 2006;8(4):315-7. doi:10.1080/14653240600855905
27. Mafi P, Hindocha S, Mafi R, Griffin M, Khan WS. Adult mesenchymal stem cells and cell surface characterization: a systematic review of the literature. Open Orthop J. 2011;5(Suppl 2):253-60. doi:10.2174/1874325001105010253
28. Mendicino M, Bailey AM, Wonnacott K, Puri RK, Bauer SR. MSC-based product characterization for clinical trials: an FDA perspective. Cell Stem Cell. 2014;14(2):141-5. doi:10.1016/j.stem.2014.01.013
29. Lv FJ, Tuan RS, Cheung KMC, Leung VYL. Concise review: the surface markers and identity of human mesenchymal stem cells. Stem Cells. 2014;32(6):1408-19. doi:10.1002/stem.1681
30. Jacobs SA, Roobrouck VD, Verfaillie CM, Van Gool SW. Immunological characteristics of human mesenchymal stem cells and multipotent adult progenitor cells. Immunol Cell Biol. 2013;91(1):32-9. doi:10.1038/icb.2012.64
31. Van Balkom BWM, Gremmels H, Giebel B, Lim SK. Proteomic signature of mesenchymal stromal cell-derived small extracellular vesicles. Proteomics. 2019;19(1-2):e1800163. doi:10.1002/pmic.201800163
32. Ramos TL, Sánchez-Abarca LI, Muntión S, Preciado S, Puig N, López-Ruano G, et al. MSC surface markers (CD44, CD73, CD90, and CD105) and immunomodulatory properties. Cell Commun Signal. 2016;14:2. doi:10.1186/s12964-016-0121-4
33. Munshi A, Mehic J, Creskey M, Gobin J, Gao J, Rigg E, et al. A comprehensive proteomics profiling identifies NRP1 as a novel identity marker of human bone marrow mesenchymal stromal cell-derived small extracellular vesicles. Stem Cell Res Ther. 2019;10:401. doi:10.1186/s13287-019-1516-2
34. Wiklander OPB, Bostancioglu RB, Welsh JA, Zickler AM, Murke F, Corso G, et al. Systematic methodological evaluation of factors influencing extracellular vesicle content and release. Front Immunol. 2018;9:1326. doi:10.3389/fimmu.2018.01326
35. Orbay H, Tobita M, Mizuno H. Mesenchymal stem cells isolated from adipose tissue: current clinical applications and prospects. Stem Cells Int. 2012;2012:461718. doi:10.1155/2012/461718
36. Via AG, Frizziero A, Oliva F. Biological properties of mesenchymal stem cells from different sources: current knowledge and future perspectives. Muscles Ligaments Tendons J. 2012;2(3):154-60
37. Théry C, Amigorena S, Raposo G, Clayton A. Isolation and characterization of exosomes from cell culture supernatants and biological fluids. Curr Protoc Cell Biol. 2006;30(1):3.22.1-3.22.29. doi:10.1002/0471143030.cb0322s30
38. D'Acunzo P, Kim Y, Ungania JM, Pérez-González R, Goulbourne CN, Levy E. Isolation of mitochondria-derived mitovesicles and subpopulations of microvesicles and exosomes from brain tissues. Nat Protoc. 2022;17(11):2517-49. doi:10.1038/s41596-022-00719-1
39. Dong L, Zieren RC, Horie K, Kim CJ, Mallick E, Jing Y, et al. Comprehensive evaluation of methods for small extracellular vesicles separation from human plasma, urine and cell culture medium. J Extracell Vesicles. 2021;10(2):e12044. doi:10.1002/jev2.12044
40. Tian Y, Ma L, Gong M, Su G, Zhu S, Zhang W, et al. Protein profiling and sizing of extracellular vesicles from colorectal cancer patients via flow cytometry. ACS Nano. 2018;12(1):671-80. doi:10.1021/acsnano.7b07782
41. Welsh JA, Arkesteijn GJA, Bremer M, Cimorelli M, Dignat-George F, Giebel B, et al. A compendium of single extracellular vesicle flow cytometry. J Extracell Vesicles. 2023;12(2):e12299. doi:10.1002/jev2.12299
42. Hu Y, Tian Y, Di H, Xue C, Zheng Y, Hu B, et al. Noninvasive diagnosis of nasopharyngeal carcinoma based on phenotypic profiling of viral and tumor markers on plasma extracellular vesicles. Anal Chem. 2022;94(27):9740-9. doi:10.1021/acs.analchem.2c01311
43. Cai N, Zhan X, Chen Y, Xue J, Chen C, Li Y, et al. Surface sialic acid detection of small extracellular vesicles at the single-particle level by nano-flow cytometry. Anal Chem. 2024;96(31):12718-28. doi:10.1021/acs.analchem.4c01763
44. Li Q, Li B, Ye T, Xu W, Yin H, Deng Z, et al. Requirements for human mesenchymal stem cell-derived small extracellular vesicles. Interdiscip Med. 2023;1:e20220015. doi:10.1002/INMD.20220015

45. Zhang X, Tang J, Kou X, Huang W, Zhu Y, Jiang Y, et al. Proteomic analysis of MSC-derived apoptotic vesicles identifies Fas inheritance to ameliorate haemophilia A via activating platelet functions. J Extracell Vesicles. 2022;11(7):e12240. doi:10.1002/jev2.12240
46. Bi Y, Qiao X, Liu Q, Song S, Zhu K, Qiu X, et al. Systemic proteomics and miRNA profile analysis of exosomes derived from human pluripotent stem cells. Stem Cell Res Ther. 2022;13(1):449. doi:10.1186/s13287-022-03142-1
47. Muhl L, Genové G, Leptidis S, Liu J, He L, Mocci G, et al. Single-cell analysis uncovers fibroblast heterogeneity and criteria for fibroblast and mural cell identification and discrimination. Nat Commun. 2020;11(1):3953. doi:10.1038/s41467-020-17740-1
48. Fernyhough ME, Okine E, Hausman G, Vierck JL, Dodson MV. PPARγ and GLUT-4 expression as developmental regulators/markers for preadipocyte differentiation into an adipocyte. Domest Anim Endocrinol. 2007;33(4):367-78. doi:10.1016/j.domaniend.2007.05.001
49. Auger C, Kajimura S. Adipose tissue remodeling in pathophysiology. Annu Rev Pathol. 2023;18:71-93. doi:10.1146/annurev-pathol-042220-023633
50. Grant D, Wanner N, Frimel M, Erzurum S, Asosingh K. Comprehensive phenotyping of endothelial cells using flow cytometry 2: Human. Cytometry A. 2021;99(3):257-64. doi:10.1002/cyto.a.24293
51. Sharma S, Cabana R, Shariatmadar S, Krishan A. Cellular volume and marker expression in human peripheral blood apheresis stem cells. Cytometry A. 2008;73(2):160-7. doi:10.1002/cyto.a.20524
52. Jakl V, Ehmele M, Winkelmann M, Ehrenberg S, Eiseler T, Friemert B, et al. A novel approach for large-scale manufacturing of small extracellular vesicles from bone marrow-derived mesenchymal stromal cells using a hollow fiber bioreactor. Front Bioeng Biotechnol. 2023;11:1107055. doi:10.3389/fbioe.2023.1107055
53. Zhang J, Rima XY, Wang X, Nguyen LTH, Huntoon K, Ma Y, et al. Engineering a tunable micropattern-array assay to sort single extracellular vesicles and particles to detect RNA and protein in situ. J Extracell Vesicles. 2023;12(11):e12369. doi:10.1002/jev2.12369
54. Kim J, Lee SK, Jung M, Jeong SY, You H, Won JY, et al. Extracellular vesicles from IFN-γ-primed mesenchymal stem cells repress atopic dermatitis in mice. J Nanobiotechnol. 2022;20:526. doi:10.1186/s12951-022-01700-8
55. Winston T, Song Y, Shi H, Yang J, Alsudais M, Kontaridis MI, et al. Lineage-specific mesenchymal stromal cells derived from human iPSCs showed distinct patterns in transcriptomic profile and extracellular vesicle production. Adv Sci (Weinh). 2024;11(28):e2308975. doi:10.1002/advs.202308975
56. Nguyen VVT, Welsh JA, Tertel T, Choo A, van de Wakker SI, Defourny KAY, et al. Inter-laboratory multiplex bead-based surface protein profiling of MSC-derived EV preparations identifies MSC-EV surface marker signatures. J Extracell Vesicles. 2024;13(6):e12463. doi:10.1002/jev2.12463